Complex remanent magnetization in the Kızılkaya Ignimbrite (Central Anatolia): implication for paleomagnetic directions

Alessandro Agrò[1,2,*], Elena Zanella[1,2], Jean-Luc Le Pennec[3], Abidin Temel[4]

1 – Dipartimento di Scienze della Terra, Via Valperga Caluso 35, 10125 Torino, Italy

2 – ALP – Alpine Laboratory of Paleomagnetism, Peveragno, Italy

3 – IRD, Laboratoire Magmas et Volcans, 5 rue Kessler, 63038 Clermont-Ferrand Cedex, France

4 – Hacettepe University, Department of Geological Engineering, 06532, Beytepe, Ankara, Turkey

*** Corresponding author: Dipartimento di Scienze della Terra, Via Valperga Caluso 35, 10125 Torino, Italy. Fax n: +390116705146; e-mail: alessandro.agro@unito.it**

E-mail addresses: alessandro.agro@unito.it; elena.zanella@unito.it; jeanluc.lepennec@ird.fr; atemel@hacettepe.edu.tr

Abstract

Volcanic rocks are invaluable materials for paleomagnetic studies, with many applications for geological and tectonic purposes. However, beyond this indisputable input, little attention has been paid to evaluating the consistency and reliability of the paleomagnetic data when results are obtained on a single volcanic unit with uneven magnetic mineralogy. This is notably the case in large-volume pyroclastic flow deposits known as ash-flow tuffs or ignimbrites, which have been widely used in previous paleomagnetic works. Here we investigate this issue and bring evidence of significant magnetic heterogeneities in ignimbrite deposits (magnetic mineralogy, susceptibility,

NRM, coercivity etc.) and we emphasize the requirement of a stratigraphic sampling strategy for these type of volcanic rocks in order to obtain reliable data. Our application concentrates on the Kızılkaya ignimbrite, the youngest large-volume unit of the Neogene ignimbrite sequence of the Central Anatolian Volcanic Province. Six sections were sampled at different stratigraphic heights within the devitrified portion of the ignimbrite. Isothermal remanence measurements point to low-Ti titanomagnetite as the main magnetic carrier at all sites; at some sites, the occurrence of oxidized Ti-magnetite and hematite is disclosed. The characteristic remanent magnetization is determined after stepwise thermal and AF demagnetization and clearly isolated by principal component analysis at most sites. Here, the site mean paleomagnetic direction is consistent with the data from the literature. At other sites, remanence is more complex: the direction moves along a great circle during demagnetization and no stable end-point is reached. The occurrence of oxidized magnetite and or hematite as well as two remanence components with overlapping coercivity and blocking temperature spectra suggest that the Kızılkaya ignimbrite acquired first a thermal remanent magnetization and then, during the final cooling or a short time later, a secondary remanent magnetization component. Notwithstanding Kızılkaya ignimbrite is a single cooling unit, its magnetic properties suffer substantial variations laterally and vertically through the deposit. The Kızılkaya case shows that thick pyroclastic deposits should be sampled according to a stratigraphic approach, at different sites and different stratigraphic heights at each individual location. Otherwise, under-sampling may significantly affect the paleomagnetic results.

Keywords: ignimbrite, magnetic remanence, Kızılkaya, Cappadocia

1. Introduction

Most volcanic rocks contain ferro- and ferri-magnetic minerals that record past geomagnetic field in both direction and intensity. Lavas and indurated or welded pyroclastic rocks thus represent an

52 invaluable material to obtain paleomagnetic information of utmost relevancy for volcanological and
53 tectonic works. A significant literature based on such studies has arisen in past decades, resulting in
54 major advances in many fields of geosciences. The applications have been especially focused on
55 stratigraphic correlations, paleogeographic reconstructions and deformation quantification at plate
56 boundaries and orogenic belts (Eldredge et al. 1985; Johnston 2001; Kent & Olsen 1997;
57 Nourgaliev et al. 2007). While the input of paleomagnetic results based on the analysis of volcanic
58 rocks is indisputable, little attention has been paid to sampling strategies and notably to the
59 evaluation of the reliability of the paleomagnetic data when results are obtained on a single volcanic
60 unit with uneven magnetic mineralogy (McIntosh 1991; Palmer et al. 1996; Paquereau-Lebti et al.
61 2008). The aim of the present study is to take a closer look to this issue by focusing on magnetic
62 properties of volcanic ash-flow tuffs, known as ignimbrites, which have been widely used in
63 previous paleomagnetic works (e.g. Black et al. 1996; Urrutia-Fucugauchi et al. 2000; Urrutia-
64 Fucugauchi & Ferrusquìa-Villafranca 2001) and for the evaluation of ignimbrite flow directions and
65 vent location (e.g. Alva-Valdivia et al. 2005; Ort et al. 1999; Palmer & MacDonald 1999; Reynolds
66 1997; Rosenbaum 1986; Schlinger et al. 1991). Recently, their potential has been also discussed for
67 paleointensity determination (Gee et al. 2010). We particularly concentrate on the magnetic
68 homogeneity of the deposit through examining the vertical variation of its magnetic properties
69 (susceptibility, coercivity and remanent magnetization) to infer the chemical and physical processes
70 that occurred at specific levels in the deposit.
71 The perspective of reliable magnetic results is supported by the fact that many Neogene and
72 Quaternary ignimbrites are well exposed over a wide area, with a well-established
73 paleotopography;in these cases geological constraints can help in reconstructing flow directions and
74 locate the vent position. Besides, welded ignimbrites are mostly characterized by a stable thermal
75 remanent magnetization (TRM), which provides an accurate paleomagnetic record.
76 Pioneering works on Köenigsberger ratio showed that the variation of the crystal properties with
77 cooling rate significantly affects the TRM acquired in a rhyolitic ignimbrite in New Zealand

78 (Hatherton 1954). In addition, Reynolds (1977) documented lateral and vertical variations of
79 paleomagnetic directions recorded in a the welded tuff of Yellowstone Group, and Rosenbaum
80 (1986) highlighted the effect of viscous deformation on remanence in some ash flow sheets of the
81 Paintbrush tuff, Nevada. Sedimentation, cooling, viscous compaction (welding), possible
82 rheomorphic creep, and other post-emplacement processes within a temperature range colder than
83 the magnetic blocking temperature can complicate the paleomagnetic record, resulting in directional
84 variations both laterally and vertically within ignimbrite deposits (Black et al. 1996; Gose 1970;
85 Schlinger et al. 1991).
86 Understanding the origin of paleomagnetic complexities in ignimbrites is important to obtain
87 improved usage of paleomagnetic directions in such deposits, and to gain insight into the processes
88 which affect the magnetic signal. In this work, we perform a detailed analysis of the paleomagnetic
89 signal in an ignimbrite unit of Cappadocia (Central Anatolia, Turkey). Earlier paleomagnetic
90 research in the area aimed at estimating tectonic rotation rates to infer recent geodynamic evolution
91 (Piper et al. 2002), but did not address intrinsic paleomagnetic variability of the ignimbrite units. On
92 the other hand, the stratigraphy and correlation pattern of the Cappadocia ignimbrites have been
93 debated in past decades because of inconsistencies among the different investigation techniques, i.e.
94 bio-stratigraphic and geochronologic datings (e.g. Pasquarè et al. 1988; Le Pennec et al. 1994;
95 Mues-Schumacher & Schumacher 1996; Temel et al. 1998; Le Pennec et al. 2005; Viereck-Goette
96 et al. 2010; Aydar et al. 2012). Here we focus on a single unit, the Kızılkaya ignimbrite, which is
97 well exposed at the top of the continental Cappadocia succession, and we investigate the magnetic
98 mineralogy and remanence patterns along selected sub-vertical profiles. The Kızılkaya ignimbrite
99 offers favorable conditions to address the issue presented above: firstly, recent analyses of zircon
100 populations from pumice and whole rock samples indicate reliable correlation of this conspicuous
101 unit (Aydar et al. 2012; Paquette & Le Pennec 2012). Secondly, the partly welded Kızılkaya
102 ignimbrite displays both lateral and vertical lithological diversity, with uneven degree of
103 mechanical and viscous compaction, and a range of alteration and weathering facies. Thirdly,

104 previous magnetic data on the Kızılkaya unit have concentrate on anisotropy of magnetic
105 susceptibility (Le Pennec et al. 1998; Le Pennec 2000), and paleomagnetic directions (Piper et al.
106 2002), but none have focused on deciphering the diversity and origin of magnetic mineralogy and
107 remanence within the deposits.
108
109 2. Geological setting
110 The Central Anatolian Volcanic Province (CAVP), a NE-SW trending Neogene-Quaternary
111 volcanic field in the Anatolian microplate, developed upon the pre-Oligocene metamorphic and
112 granitic basement (Toprak et al. 1994) (Fig. 1). The CAVP is characterized by a compositional
113 trend from initial calc-alkaline signatures to quaternary alkaline affinities, and has been correlated
114 to the extensional deformation of the Central Anatolian block, in a context of regional convergence
115 between Eurasia and Afro-Arabia since the latest Mesozoic (Faccenna et al. 2003; Dilek 2010).
116 The CAVP consists of many Quaternary monogenetic edifices and a few elevated strato-volcanoes
117 (Hasan and Erciyes, Fig. 1) and exposes a succession of widespread Neogene ignimbrite units
118 intercalated with continental deposits. The late Miocene Kızılkaya ignimbrite is the youngest large-
119 volume unit of the Cappadocia Plateau sequence; recent ^{39}Ar-^{40}Ar and U-Pb determinations on
120 minerals yield an eruption age of ~5.4 Ma (Aydar et al. 2012; Paquette & Le Pennec 2012), and
121 detailed widespread sampling argues for robust correlation across the whole Cappadocia Plateau.
122 The >180 km^3, low aspect-ratio Kızılkaya ignimbrite defines flat structural surfaces on the plateau
123 and usually occurs as a 10-30 m-thick sheet (locally > 80 m), red-tinted and columnar-jointed unit
124 (Pasquarè et al. 1988). In the eastern part of the Plateau, the ignimbrite is underlain by a plinian
125 pumice-fall deposit (Le Pennec et al. 1994; Schumacher & Mues-Schumacher 1996). The
126 ignimbrite is commonly welded and sintered and the degree of welding varies both vertically and
127 laterally, with eutaxitic textures observed in some valley-ponded facies (e.g. Ihlara, Soğanlı). The
128 jointing pattern indicates that it is a simple cooling unit, with two distinct layers corresponding to a
129 lower grayish vitric zone and an upper reddish devitrified zone. Inverse grading of pumice clasts is

130 locally observed, and accidental (lithic) clasts are common and generally oxidized. Pumice are
131 porphyritic (~30-35% phenocrysts), rhyolitic in composition (71-74 % SiO_2), and host a mineral
132 assemblage of plagioclase, biotite, some quartz and amphibole, and minor amounts of magnetite
133 and ilmenite (Temel et al. 1998; Le Pennec et al. 1998; Viereck-Goette et al. 2010).
134
135 3. Sampling and laboratory methods
136 Paleomagnetic sampling was performed at 6 localities, namely Akköy, Güzelöz, Ihlara, Soğanlı,
137 Tilköy, and Yesilöz (Fig. 1). At each locality, we selected natural and man-made (road-cuts and
138 quarries) sections to sample the deposit along subvertical profiles with limited lateral offset, using
139 an electric-powered drill to core the ignimbrite at different stratigraphic heights (2 to 9 sites along a
140 single profile), usually within the devitrified portion of the deposit (Fig. 2). Distances between the
141 sites were measured in the field using a 3-m-long graduated measuring-tape. The coring sites are
142 typically 2 – 3 m in length-width, with an inter-site distance in the range of 1 – 15 m (Fig. 1b). The
143 uniformity of sampling and the spacing between sampling sites was strongly affected by the nature
144 of the exposures (evidence of weathering or fractures and rock suitability to be cored). At each site,
145 we collected 5 to 17 cores, which were oriented using both magnetic and (when possible) solar
146 compasses, and applying a correction of +5° to each core to account for a measured magnetic
147 declination of 5°E, consistent with IGRF2010 reference field (online calculator at
148 http://www.ngdc.noaa.gov).
149 Sample preparations and magnetic measurements were performed at Alpine Laboratory of
150 Paleomagnetism (ALP, Peveragno, Italy). The cores were cut to standard cylindrical segments (25
151 mm in diameter and 23 mm in lenght), yielding a total of 444 specimens. Before magnetic
152 measurements, we weighed all the specimens to compute their density. The magnetic susceptibility
153 and its anisotropy (AMS) were first measured using a KLY-3 kappa-bridge, then, natural (NRM)
154 and isothermal (IRM) remanent magnetizations were measured using JR-5 and JR-6 spinner
155 magnetometers. At least 3-4 pilot specimens for each site were thermally and AF demagnetized at

156 10-15 steps up to a temperature of 580-600 °C and peak-field of 100 mT, respectively. No thermal
157 demagnetization was possible for Yeşilöz samples, because the specimens exploded at about 350
158 °C. The results suggested demagnetizing the remaining specimens by AF method, at 4-5 steps,
159 between 10 and 60 mT.
160 IRM acquisition and back-field measurements and thermal demagnetization of the IRM components
161 (Lowrie 1990) were obtained on at least one specimen per site. IRM acquisition curves were
162 analyzed by the method of Kruiver et al. (2001), which leads to distinguish the different
163 components in a magnetic mineral assemblage, taking into account three main parameters: the
164 saturation magnetization (SIRM), the magnetic field required to reach half of the SIRM ($B_{1/2}$), and
165 the dispersion of the distribution (DP). Besides, IRM measured at applied field of 1 T, 0.1 T, 0.3 T
166 are used to compute S-ratios at 0.1 and 0.3 T ($S_{-0.1\ T}$ = -$IRM_{-0.1T}$/ $SIRM_{1T}$; $S_{-0.3\ T}$ = -$IRM_{-0.3T}$/
167 $SIRM_{1T}$) (Thompson & Oldfield 1986). Finally, we measured the anisotropy of isothermal remanent
168 magnetization (AIRM) of selected samples from the Soğanlı section.
169
170 4. Results
171 4.1 Magnetic mineralogy
172 Thermal demagnetization of the IRM components shows dominant low and medium coercivity
173 components. The maximum blocking temperature is mainly around 560-580 °C, up to 650 °C.
174 These results point to low-Ti titanomagnetite (Fig. 3) as the main ferromagnetic mineral in the
175 Kızılkaya ignimbrite, locally associated to a high coercivity phase, probably oxidized magnetite
176 and/or hematite (Fig. 3).
177 To better resolve the occurrence of different magnetic phases at site level, we use the cumulative
178 log-Gaussian analysis proposed by Kruiver et al. (2001) for the IRM acquisition data. Magnetic
179 mineral assemblage can be distinguished in three different types (Fig. 4):
180 1. A single low-coercivity phase, which saturates at low field (0.1 – 0.3 T) and shows low values of
181 the coercivity of remanence B_{cr}, ranging from 20 to 40 mT. It is highlighted by the presence of a

182 single ferrimagnetic component in the Linear, Gradient and Standardized Acquisition Plot
183 (LAP, GAP, SAP) (Fig. 4a). This phase is interpreted as Ti-magnetite. It is present at all
184 localities: at Güzelöz, Tilköy, the lower part of Akköy and in the upper half part of Ihlara
185 section it is the only component. A special case is Yeşilöz, where Ti-magnetite is associated to
186 an iron sulfide mineral.
187 2. Two magnetic phases (Fig. 4b), both with low- to medium-coercivity. One has the same
188 characteristics described in point 1). The second saturates at higher fields (< 1 T); B_{cr} values
189 range from 50 to 100 mT. These results suggest Ti-magnetite plus oxidized Ti-magnetite, as
190 also pointed out by thermal demagnetization of IRM (Fig. 3b). Soğanlı, the basal portion of the
191 ignimbrite at Ihlara, and the upper portion at Akköy, typically show the presence of these
192 phases.
193 3. Three magnetic phases. The occurrence of a high-coercivity component, not saturated by fields <
194 1.5 T, whose B_{cr} values are high, mainly ranging from 100 to 200 and in one case up to 400 mT
195 (Fig. 5) reveals the presence of a minor amount of hematite (Fig. 4c). This behaviour is
196 characteristic of the upper part of Soğanlı section. Here, from the base to the top of the deposit,
197 all magnetic parameters point out to an increasing effect of oxidation processes: at the base, we
198 only found Ti-magnetite (B_{cr} = 30-40 mT, Median Destructive Field (MDF) = 30 mT), then also
199 oxidized Ti-magnetite (B_{cr} = 50-60 mT, MDF = 40-50 mT), and in the upper part hematite is
200 present (B_{cr} = 100-400 mT, MDF > 60 mT). The top of the Akköy section falls as well within
201 this type.
202 Both S-ratio at 0.1 and 0.3 T are computed to assess the relative contribution of high- versus low-
203 coercivity components. Normally computed for marine sediments, S-ratios were used by Sweetkind
204 et al. (1993), for the Carpenter Ridge Tuff, Colorado, for the definition of different oxide groups,
205 resulting from hydrothermal alteration. For Kızılkaya, in the 60% of the sites, $S_{-0.3\ T}$ is higher than
206 0.9; in the remaining sites the $S_{-0.3\ T}$ drops to 0.3 and varies mainly between 0.3 and 0.5. The
207 variation of both B_{cr} and $S_{-0.3\ T}$ ratio as a function of the stratigraphic height is displayed in figure 5;

208 the grey area indicates the typical range of variability associated with the presence of Ti-magnetite.
209 $S_{-0.1T}$ is more variable, ranging from -0.16 to 0.84, its value being also affected by the ferrimagnetic
210 grain-size (Kruiver et al. 2001).
211 No correlation between oxidation and deposit stratigraphic height, is possible. Only on four out of
212 six localities the base contact of the ignimbrite deposits crops out (Fig. 1b) and only at one locality,
213 the top contact is observed.
214 On the whole, these results are consistent with those of the thin section analyses (Le Pennec et al.
215 1998), which showed abundant equant to elongate Fe-oxide grains, typically 50 to 400 μm in size.
216 They suggested the presence of multidomain (MD) magnetite, but also recognized some small
217 magnetite crystals included in biotite and apatite. Piper et al. (2002) report values from 0.07 to 0.11
218 for the ratio between the saturation remanent magnetization and the saturation magnetization
219 (M_{rs}/M_s). They confirm the occurrence of dominant MD grains, plus a small fraction (~10 – 30%)
220 of single-domain (SD) grains.
221 Bulk susceptibility varies between 100 and 10,000 μSI. Depending on the locality, stable and
222 relatively high values of susceptibility are observed through the deposit, as at Ihlara, Yeşilöz, and
223 Tilköy; conversely, at Akköy and Soğanlı, susceptibility values decrease upward in the section. We
224 relate this trend to the occurrence of oxidation, revealed by the presence of magnetic phases
225 characterized by higher B_{cr} and lower $S_{-0.3\ T}$ values (Fig. 5). The density varies from 1.1 to 2.4
226 g/cm^3. Magnetic susceptibility and density vary with the degree of welding compaction with a
227 positive linear trend (Fig. 6). Le Pennec et al. (1998) distinguished two groups: one, characterized
228 by density and susceptibility values higher than 1.5 g/cm^3 and 3000 μSI, respectively, as
229 representative of non-altered ignimbrite; the other, with lower values, is affected by hydrothermal
230 alteration and weathering. Here, low susceptibility values are independent of density and are
231 associated with the occurrence of haematite at Soğanlı and Akköy. This continuous trend of density
232 vs. magnetic susceptibility suggests a possible bias in the sampling protocol of Le Pennec et al.
233 (1998), and is resolved in our sampling strategy through systematic vertical coring.

234

235 4.2 Magnetic remanence

236 NRM intensity varies over one order of magnitude in the range 0.2 – 2.4 A/m, and the highest
237 values occur in the specimens from the most welded sites, e.g. at Ihlara. For most sites, during AF
238 demagnetization, the direction changes very little in the first steps below 200 mT, and then does not
239 change any more (Fig. 7a). Thermal demagnetization reveals two components: a high-T_b
240 component, pointing to the origin (Fig. 7b) and a low-T_b component (20 – 400 °C). This latter
241 shows a small angular deviation with respect to the high-T_b component, generally within 5° and it is
242 deflected towards both E and W. These results show that the NRM consists of a negligible
243 secondary component, likely viscous in origin, and a stable characteristic component (ChRM) of
244 reverse polarity, which is well-defined, with maximum angular deviation (MAD) values typically
245 lower than 4°. The ChRM directions are well clustered (Fig. 8a, b) and their site mean values,
246 computed using Fisher's (1953) statistics, yield semi-angles of confidence α_{95} comprised mainly
247 between 1.5° and 5°

248 At some sites, the remanent magnetization is more complex, as evidenced in most specimens by no
249 stable end-point direction reached during AF or thermal demagnetization, and the resulting
250 remanence directions, measured after each demagnetization step, moving along a great circle (Fig.
251 7c, d). The NRM consists of two components with overlapping coercivity or unblocking
252 temperature spectra. This is observed in figure 7c, where the intensity decay of the specimen is
253 rather slow and the Median Destructive Field (MDF) is very high. The unblocking temperature
254 spectra of the two remanence components (Fig. 7d) apparently overlap completely. For these sites,
255 we computed the site mean direction using the great circle remagnetization paths and Fisher's
256 statistics as modified by McFadden & McElhinny (1988). Also in this case, the ChRM directions
257 are clustered and their site mean value well defined, with α_{95} below 5° (Fig. 8c, d; Table 1).

258 A closer inspection in the arrangement of the ChRM directions at site level shows that their
259 distribution is elongated (Fig. 9 as well as in Fig. 8b, d) and the circular distribution, as assumed by

Fisher's statistics, is rather uncommon. The eccentricity in the distribution was computed following Engebretson & Beck (1978). Its value is 0 for a circular distribution, 1 for an elliptical one. In 14 out of 33 sites, the eccentricity is higher than 0.80 and mostly in the range 0.90 – 0.95. Besides, directions appear to spread over a plane and it is possible to compute a best-fitting great circle, whose pole is well-defined with a confidence limit below 15° (Fig. 9). Samples from these sites hold two magnetization components, which are not resolved after the demagnetization treatment. For those sites, no mean site paleomagnetic direction is provided in table 1. Instead, the remagnetization circles were used. Thus the mean paleomagnetic direction for the Kızılkaya ignimbrite is computed using both 19 mean site directions and 14 best-fitting great circles, as illustrated in Fig. 10, yielding D = 179.5°, I = -42.9°, k = 93, α_{95} = 2.6°.

5. Discussion

The emplacement of large-volume ignimbrites and the deposition of accompanying plinian tephra fallout occur instantaneously at geological time scales. Widespread ignimbrite deposits might thus be considered as ideal stratigraphic marker horizons at the regional scale, as often reported in literature (Best et al. 1995; Bogue & Coe 1981; McIntosh 1991; Ort et al. 1999; Paquereau-Lebti et al. 2008). In these cases, the correlation is straightforwardly applied with little attention to the intrinsic characteristics of the deposit as well as the processes that acted at a specific locality.

Various processes have been proposed in the literature to explain lateral and vertical variations of the paleomagnetic direction recorded in an ignimbrite: reheating by an overlying hot flow deposit (Gose 1970); overprinting of the primary thermoremanence by a later chemical remanent magnetization (CRM) (Reynolds 1977), sub-blocking temperature plastic deformation (Rosenbaum 1986), but also welding compaction, anisotropy of magnetic susceptibility, geomagnetic secular variations, local magnetic anomalies, inexact bedding tilt corrections, and tectonic tilting, as pointed out by Rosenbaum (1986). Secondary alteration and formation of ferromagnetic grains with

285 unblocking temperatures of ChRM above emplacement temperatures may occur during
286 devitrification or vapor-phase crystallizations (Paquereau-Lebti et al. 2008).
287 Although The Kızılkaya ignimbrite is a single flow and cooling unit, its magnetic properties show
288 notable variations within the deposit. In most places the magnetic mineralogy is not vertically
289 homogeneous, as might be expected from a large-volume pyroclastic flow emplaced in a short time
290 interval. Notably, the magnetic susceptibility values display considerable differences among sites in
291 the same section, and at some locations the magnetic remanence varies significantly from lower to
292 upper sites. The necessity of a stratigraphic sampling in order to obtain reliable data for
293 paleomagnetic reconstructions is therefore of primary importance.
294 Figure 11 shows the variations of the site paleomagnetic direction throughout the section at each
295 locality. At Akköy, Güzelöz, Tilköy and Yeşilöz, the directions show negligible variations. At
296 Soğanlı, and to a minor extent at Ihlara, the paleomagnetic directions vary significantly with the
297 stratigraphic height: declination ranges from 170° to 210°, inclination from -34° to -55°. Large
298 deflections from the mean direction occur at sites characterized by the occurrence of oxidized
299 magnetite and/or hematite. A partial to complete secondary magnetic overprint partially masks the
300 primary remanence. These results suggest that at these sites the Kızılkaya ignimbrite acquired a
301 thermal remanent magnetization during the emplacement and a chemical remanent magnetization,
302 during the eventual cooling or a short time later, which possibly resides in the higher coercivity
303 magnetic phases (i.e. oxidized magnetite and haematite). Alva-Valdivia et al. (2001) detected in the
304 iron ores and associated igneous rocks in the Cerro Mercado (Mexico) the presence of a pervasive
305 CRM replacing completely or partially an original TRM, and related it to thermo-chemical
306 processes due to hydrothermalism which occurred during or soon after extrusion and cooling of the
307 magma. They recognized two magnetization components with overlapping unblocking temperature
308 spectra: a high temperature component, and a low temperature component corresponding to
309 chemical overprint carried by hematite resulting from partial martitization of original magnetite (an
310 oxidation process leading to maghemite and followed by inversion of maghemite to hematite).

311 McClelland-Brown (1982), interpreted the T_b overlapping during thermal demagnetization as a clue
312 for the occurrence of two probably contemporaneous thermal and chemical magnetizations;
313 consistently, Piper et al. (2002) recognized in the Kızılkaya ignimbrite two magnetization
314 components, thermal and thermo-chemical (TCRM) in origin. They interpreted the low-blocking
315 temperature reverse component as primary TRM and the high-blocking temperature component as a
316 secondary chemical (CRM) or thermochemical (TCRM) remanence acquired in younger geological
317 times. This interpretation is supported by the angular difference between the two components,
318 which would result from tectonic rotations which affected the area.
319 Our data show that the angular deviation is not systematic, because the low-T_b component in some
320 cases is deviated towards E, in other towards W. Moreover, AF demagnetizations reveal only one
321 well-defined component. In the case of Akköy, site KZ7-3, for example, the mean direction
322 computed for AF directional data is D = 176.8°, I = -31.9°, α_{95} = 3.0°. The high-T_b component (D =
323 177.3°, I = -30.3°, Fig. 7b) falls within the α_{95} semi-cone of confidence. It may therefore be
324 reasonably assumed as the primary remanence. On the contrary, the low-T_b component (D = 172.1°,
325 I = -34.4°) falls outside the confidence limit and the small angular deviation between the two
326 remanences (ca 6°) is fully consistent with the effect of paleosecular variations. According to our
327 interpretation, the low-Tb component would have been acquired a short time after the emplacement.
328 Paleomagnetic directions recorded in the Kızılkaya ignimbrite at some localities are well defined
329 and consistent with those of Piper et al. (2002). This is the case at Akköy, Güzelöz and Yeşilöz,
330 where mean paleomagnetic directions (n = 12, D = 175.2°, I = -38.6°, k = 249, α_{95} = 2.7°) are
331 statistically indistinguishable from literature data (D = 170.9°, I = -39.9°; k = 211, α_{95} = 5.3°),
332 because their 95% confidence ellipses intersect. In these cases, the Kızılkaya ignimbrite possesses a
333 single and stable direction of thermal remanence, which from all evidence appears to be a reliable
334 representation of the ambient field at the time of cooling (Fig. 11).
335 A different behavior characterizes the remaining localities, where the remanent directions change
336 systematically with stratigraphic height. In 14 out of 33 cases, the ignimbrite is characterized by

two remanence components, as a result of the complex magnetic mineralogy (occurrence of Ti-magnetite, oxidized Ti-magnetite and hematite) and variations in the thermal cooling and alteration histories. Depending on the temperature and coercivity spectra of the magnetic carriers it is not always possible to resolve the magnetization components. If the secondary components are not completely erased, the paleomagnetic results are biased, as shown by the elliptical distribution of the ChRM directions (Fig. 9). In these sites, ChRMs are arranged along a great circle and no mean direction was computed. Instead, we calculated the pole of the best-fitting circle for each of the 14 sites, and the resulting mean paleomagnetic direction for Kızılkaya ignimbrite was obtained combining both the stable directions and the best-fitting circles (Fig. 10). Where present, the secondary overprint contributes to deflect the direction by a few degrees. The Kızılkaya mean paleomagnetic direction obtained here and by Piper et al. (2002) are 7.4° apart, even if their confidence ellipses intersect (Fig. 10). The difference is smaller for the inclination, but it should be treated with caution when interpreting tectonic rotations in young rocks, because the uncertainty associated to the rotation (ΔR) (Demarest 1983) may be higher than the rotation (R). Piper et al. (2002) identified a generalized anticlockwise rotation for the Cappadocian ignimbrites younger than 9 Ma with respect to Eurasian and African palaeofields. In the Cappadocian sector they estimated the rotation rate at 9 +/- 5°.

The inclination values are systematically lower than GAD for both this study and Piper et al. (2002). The difference with respect to GAD is -15° and -18°, respectively. The paleomagnetic direction that we inferred at Akköy, Güzelöz and Yeşilöz shows an inclination in agreement with that of Piper et al. (2002). These authors discussed some possibilities to explain the ΔI. They excluded experimental problems and imperfections in the references APWPs (Apparent Polar Wander Patterns), but took into account the occurrence of a complex geomagnetic source during the rock's magnetization acquisition and a northwards movement of the region since the time of magnetization. In the sites where a complex magnetization is revealed and two components are recognized, inclination values are higher, up to -55° and closer to the GAD one: we suggest that

these higher values are associated with the secondary chemical remanence. Since the two components were acquired close in time, a hypothesis is that the inclination of the secondary component represents a reliable record of the Earth's magnetic field during emplacement/alteration. Yet, this component shows a low intensity, thus in the average the thermal remanence is prevalent and the result is characterized by a low inclination value. The latter may reveal the occurrence of some processes acting soon after emplacement that bias the recorded magnetic direction.

Magnetic anisotropy can affect the recorded field toward the plane of maximum alignment of the magnetic grains, and anisotropy of remanence may lead to apparent paleosecular variation (Gattacceca & Rochette 2002). To test the flattening effect we measured the anisotropy of isothermal remanent magnetization (AIRM) for Soğanlı specimens at sites KZ2-1, KZ2-3 and KZ5-5. Data are preliminary; the anisotropy degree P_{AIRM} is around 1.200. Using the relation $\tan I_r = (1/P_{AIRM})\tan I_g$, where I_r and I_g are respectively the paleomagnetic inclination recorded by the rocks and the inclination of the paleofield during cooling, an inclination $I_r \sim 53°$ is determined. This value is still lower (-5°) than the expected one, but it may explain part of the discrepancy. Possibly it may be added to other mechanisms as for example in Piper et al. (2002): a regional effect which affects the eastern Mediterranean, the northward movement of the Central Anatolian block.

6. Conclusion

This study provides a detailed investigation of the factors influencing the paleomagnetic signal in the widespread, partly welded Kızılkaya ignimbrite in Central Anatolia. Magnetic remanences are not vertically homogenous through the deposits. Two main cases are distinguished:

1. A stable and well-defined TRM, whose direction is consistent with previous literature data (Piper et al. 2002), that is detected in at sites where Ti-magnetite (or weakly oxidized-magnetite) is the only magnetic career.

2. Two magnetization components, with overlapping T_b e coercivity spectra. This case is typically found where magnetic mineralogy is given by Ti-magnetite, oxidized Ti-magnetite and hematite.

We suggest the occurrence of a primary TRM and a secondary CRM acquired a short time later, and their angular difference is consistent with the paleosecular variation.

The Kızılkaya mean paleomagnetic direction shows a significant difference in the inclination value with that expected for GAD in the region. We tentatively attributed part of this difference to compaction processes which acted during ignimbrite cooling.

In summary, the Kızılkaya case study indicates that thick ignimbrite units should not be considered as magnetically uniform rock bodies. Detailed and systematic sampling is required to evidence possible rock-magnetic inhomogeneity, avoiding local and inadequate sampling which may lead to unrepresentative paleomagnetic results. Hence, sampling of ignimbrite sheets should be carried out both laterally and vertically to account for possible influences of overlapping thermal and chemical processes in controlling the remanence, and paleomagnetic results should be interpreted with caution for volcanological, tectonic and geodynamic applications.

Acknowledgments

Roberto Lanza is thanked for his thorough review of an earlier version of this manuscript.

References

Alva-Valdivia, L.M., Goguitchaichvili, A., Urrutia-Fucugauchi, J., Caballero-Miranda, C & Vivallo, W., 2001. Rock-magnetism and ore microscopy of the magnetite-apatite ore deposits from Cerro de Mercado, Mexico. Earth Planet Sp., 53, 181—192.

Alva-Valdivia, L.M., Rosas-Elguera, J., Bravo-Medina, T., Urrutia-Fucugauchi, J., Henry, B., Caballero, C., Rivas-Sanchez, M.L., Goguitchaichvili, A. & López-Loera, H., 2005.

412 Paleomagnetic and magnetic fabric studies of the San Gaspar ignimbrite, western Mexico-
413 constraints on emplacement mode and source vents. J. Volcanol. Geotherm. Res., 147, 68--80.
414 Aydar, E., Schmitt, A.K., Çubukçu, H. E., Akin, L., Ersoy, O., Sen, E., Duncan, R. A. & Atici, G.,
415 2012. Correlation of ignimbrites in the central Anatolian volcanic province using zircon and
416 plagioclase ages and zircon compositions, J. Volcanol. Geotherm. Res., 213-214, 83--97.
417 doi:10.1016/j.jvolgeores.2011.11.005
418 Best, M.G., Christiansen, E.H., Deino, A.L., Grommé, C.S. & Tingey, D.G., 1995. Correlation and
419 emplacement of a large, zoned, discontinuously exposed ash flow sheet: The $^{40}Ar/^{39}Ar$
420 chronology, paleomagnetism, and petrology of the Pahranagat Formation, Nevada, J. Geophys.
421 Res., 100, 24593--24609.
422 Black, T.M., Shane, P.A.R., Westgate, J.A. & Froggatt, P.C., 1996. Chronological and
423 paleomagnetic constraints on widespread welded ignimbrites of the Taupo Volcanic Zone, New
424 Zealand. Bull. Volcanol., 58, 226--238.
425 Bogue, S.W. & Coe, R.S., 1981. Paleomagnetic correlation of Columbia River Basalt Flow using
426 secular variation, J. Geophys. Res., 86, 11883--11897.
427 Demarest, H.H., 1983. Error analysis for the determination of tectonic rotation from palaeomagnetic
428 data, J. Geophys. Res. 88, 4321--4328.
429 Dilek, Y., 2010. Eastern Mediterranean geodynamics, Int. Geol. Rev., 52, 111--116.
430 Eldredge, S., Bachtadse, V. & Van der Voo; R., 1985. Paleomagnetism and the orocline hypothesis,
431 Tectonophysics., 119, 153--179.
432 Engebretson, D.C. & Beck, M.E., 1978. On the shape of directional data sets, J. Geophys. Res., 83,
433 5979--5982.
434 Facenna, C., Jolivet, L., Piromallo, C. & Morallo, A., 2003. Subduction and the depth of convection
435 in the Mediterranean mantle, J. Geophys. Res., 108, 2099, doi: 1029/2001JB001690.
436 Fisher, R.A., 1953. Dispersion on a sphere, Proc. R. Soc., 217, 295--305.

437 Gattacceca, J. & Rochette, P., 2002. Pseudopaleosecular variation due to remanence anisotropy in a
438 pyroclastic flow succession, Geophys. Res. Lett., 29, 10.1029/2002GL014697
439 Gee, J.S., Yu, Y. & Bowles, J., 2010. Paleointensity estimates from ignimbrites: An evaluation of
440 the Bishop Tuff. Geochemistry, Geophysics, Geosystem, 11, Q03010,
441 doi:10.1029/2009GC002834
442 Gose, W.A., 1970. Paleomagnetic studies of Miocene ignimbrites from Nevada, Geophys. J. R.
443 Astron. Soc., 20, 241--252.
444 Hatherton, T., 1954. The permanent magnetisation of horizontal volcanic sheets, J. Geophys. Res.,
445 59, 223--232.
446 Johnston, S.T., 2001. The Great Alaskan Terrane Wreck: reconciliation of paleomagnetic and
447 geological data in the northern Cordillera, Earth and Planetary Science Letters., 193, 259--272.
448 Kent, D.V. & Olsen, P.E., 1997. Paleomagnetism of Upper Triassic continental sedimentary rocks
449 from the Dan River–Danville rift basin (eastern North America), Geological Society of America
450 Bulletin., 109, 366--377.
451 Kruiver, P.P., Dekkers, M.J. & Heslop, D., 2001. Quantification of magnetic coercivity components
452 by the analysis of acquisition curves of isothermal remanent magnetisation, Earth Planet. Sci.
453 Lett., 189, 269--276.
454 Le Pennec, J.-L., 2000. Identifying ash flow sources with directional data: An application to the
455 Kizilkaya ignimbrite, central Anatolia, J. Geophys. Res., 105, 28427--28441.
456 Le Pennec, J.-L., Bourdier, J.-L., Froger, J.-L., Temel, A., Camus, G. & Gourgaud, A., 1994.
457 Neogene ignimbrites of the Nevşehir plateau (central Turkey): stratigraphy, distribution and
458 source constraints, J. Volcanol. Geotherm. Res. 63, 59--87.
459 Le Pennec, J.-L., Chen, Y., Diot, H., Froger, J.-L. & Gourgaud, A., 1998. Interpretation of
460 anisotropy of magnetic susceptibility fabric of ignimbrites in terms of kinematic and
461 sedimentological mechanisms: An Anatolian case-study, Earth Planet. Sci. Lett. 157, 105--127.

462 Le Pennec, J.-L., Temel, A., Froger, J.-L., Sen, S., Gourgaud, A. & Bourdier, J.-L., 2005.
463 Stratigraphy and age of the Cappadocia ignimbrites, Turkey: reconciling field constraints with
464 paleontologic, radiochronologic, geochemical and paleomagnetic data, J. Volcanol. Geotherm.
465 Res., 141, 45--64.
466 Lowrie, W., 1990. Identification of ferromagnetic minerals in a rock by coercitivity and unblocking
467 properties, Geophys. Res. Lett. 17, 159--162.
468 McClelland-Brown, E., 1982. Discrimination of TRM and CRM by blocking-temperature spectrum
469 analysis, Phys. Earth Planet. Int., 30, 405--414.
470 McFadden, P.L. & McElhinny, M.W., 1988. The combined analysis of remagnetization circles and
471 direct observations in palaeomagnetism, Earth Planet. Sci. Lett., 87, 161--172.
472 McIntosh, C.W., 1991. Evaluation of paleomagnetism as a correlation criterion for Mogollon-Datil
473 Ignimbrites, Southwestern New Mexico, J. Geophys. Res., 96, 13459--13483.
474 Nourgaliev, D.K., Yasonov, P.G., Oberhaensli, H., Heller, F., Borisov A.S., Chernova, I.Y.,
475 Akdasov, E.I. & Burov, B.V., 2007. Paleomagnetic Correlation of Sedimentary Sequences: The
476 Use of Secular Geomagnetic Variations for the Differentiation and Correlation of Holocene Aral
477 Sea Deposits, Physics of the Solid Earth., 43, 836--843.
478 Ort, M.H., Rosi, M. & Anderson, C.D., 1999. Correlation of deposits and vent locations of the
479 proximal Campanian Ignimbrite deposits, Campi Flegrei, Italy, based on natural remanent
480 magnetization and anisotropy of magnetic susceptibility characteristics, J. Volcanol. Geotherm.
481 Res., 91, 167--178.
482 Palmer, H.C., MacDonald, W.D., Gromme, C.S. & Ellwood, B.B., 1996. Magnetic properties and
483 emplacement of the Bishop tuff, California, Bull. Volcanol., 58, 101--116.
484 Palmer, H.C. & MacDonald, W.D., 1999. Anisotropy of magnetic susceptibility in relation to
485 source vent of ignimbrites: empirical observations, Tectonophys., 307, 207--218.
486 Paquette, J.L. & Le Pennec, J.L., 2012. 3.8 Ga-old zircons sampled by ignimbrite eruptions in Central
487 Anatolia, *Geology*. Doi:10.1130/G32472.1

488 Paquereau-Lebti, P., Fornari, M., Roperch, P., Thouret, J.-C. & Macedo, O., 2008. Paleomagnetism,
489 magnetic fabric, and $^{40}Ar/^{39}Ar$ dating of Pliocene and Quaternary ignimbrites in the Arequipa
490 area, southern Peru, Bull. Volcanol., 70, 977-997, DOI 10.1007/s00445-007-0181-y
491 Pasquarè, G., Poli, S., Vezzoli, L. & Zanchi, A., 1988. Continental arc volcanism and tectonic
492 setting in central Anatolia, Turkey, Tectonophys., 14, 217--230.
493 Piper, J.D.A., Gürsoy, H. & Tatar, O., 2002. Palaeomagnetism and magnetic properties of the
494 Cappadocian ignimbrite succession, central Turkey and Neogene tectonics of the Anatolian
495 collage, J. Volcanol. Geotherm. Res., 117, 237--262.
496 Reynolds, R.L., 1977. Paleomagnetism of Welded Tuffs of the Yellowstone Group, J. Geophys.
497 Res., 82, 3677--3693.
498 Rosenbaum, J.G., 1986. Paleomagnetic directional dispersion produced by plastic deformation in a
499 thick Miocene welded tuff, Southern Nevada: Implications for welding temperatures, J.
500 Geophys. Res., 91, 12817--12834.
501 Schlinger, C.M., Veblen, D.R. & Rosenbaum, J.G., 1991. Magnetism and Magnetic Mineralogy of
502 Ash Flow Tuffs from Yucca Mountain, Nevada, J. Geophys. Res., 96, 6035--6052.
503 Schumacher, R. & Mues-Schumacher, U., 1996. The Kızılkaya ignimbrite – an unusual low-aspect-
504 ratio ignimbrite from Cappadocia, central Turkey, J. Volcanol. Geotherm. Res., 70, 107--121.
505 Sweetkind, D.S., Reynolds, R.L., Sawyer D.A. & Rosenbaum, J.G., 1993. Effects of hydrothermal
506 alteration on the magnetization of the Oligocene Carpenter Ridge Tuff, Bachelor Caldera, San
507 Juan Mountains, Colorado, J. Geophys. Res., 98, 6255--6266.
508 Temel, A., Gündoğdu, M.N., Gourgaud, A. & Le Pennec, J.L., 1998. Ignimbrites of Cappadocia
509 (Central Anatolia, Turkey): petrology and geochemistry, J. Volcanol. Geotherm. Res., 85, 447--
510 471.
511 Thompson, R. & Oldfield, F., 1986. Environmental magnetism, Allen & Unwin, London, 227 pp.
512 Toprak, V., Keller, J., R., Schumacher, R., 1994. Volcano-tectonic features of the Cappadocian
513 volcanic province. International Volcanological Congress Excursion Guide, Ankara, 58 pp.

514 Urrutia-Fucugauchi, J., Alva Valdivia, L.M., J. Rosas Elguera, J., Campos Enríquez, O.,
515 Goguitchaichvili, A., Soler Arechalde, A.M., C. Caballero Miranda, C., Venegas Salgado, S. &
516 Sánchez Reyes, S., 2000. Magnetostratigraphy of the volcanic sequence of Río Grande de
517 Santiago-Sierra de la Primavera region, Jalisco, western Mexico, Geofisica International., 39,
518 247--265.
519 Urrutia-Fucugauchi, J. & Ferrusquìa-Villafranca, I., 2001. Paleomagnetic results for the Middle-
520 Miocene continental Suchilquitongo Formation, Valley of Oaxaca, southeastern Mexico,
521 Geofisica International., 40, 191--205.
522 Viereck-Goette, L., Lepetit, P., Gürel, A., Ganskow, G., Çopuroğlu, I. & Abratis, M., 2010. Revised
523 volcanostratigraphy of the Upper Miocene to Lower Pliocene Ürgüp Formation, Central
524 Anatolian volcanic province, Turkey. In Gropelli, G., Goette-Viereck, L. (eds.) Stratigraphy
525 and geology of volcanic areas. Geological Society of America Special Paper 464, 85-112. doi:
526 10.1130/2010.2464(05).
527 Zijderveld, J.D.A., 1967. A.C. demagnetization of rocks: analysis of results. Methods in
528 paleomagnetism, Elsevier, 254--268.
529
530 Figure caption
531 **Figure 1.** a) Schematic map of the Nevşehir plateau in the Central Anatolian Volcanic Province
532 (CAVP), contour lines = 500 m, square = sampled locality. The grey area represents the inferred
533 vent position (after Le Pennec et al., 2005). Insert: tectonic sketch map of Anatolia plate.
534 Acronyms: NAFZ/EAFZ = North/East Anatolian Fault Zone; KEF = Kırıkkale-Erbba Faul; AF =
535 Almus Fault; SLF = Salt Lake Fault; EFZ = Ecemiş Fault Zone; DSFZ = Death Sea Fault Zone;
536 BSZ = Bitilis Suture Zone; b)Stratigraphic variation of the Kızılkaya ignimbrite facies and vertical
537 distribution of sample sites (dots) in the six stratigraphic sections.
538 Figure 2. Example of a sampled stratigraphic section (Tilköy). a) sampled sites; b) typical sampled
539 facies at site KZ3-3.

Figure 3. Thermal demagnetization of the IRM components, after Lowrie (1990). In a) a specimen from Tilköy; in b) a specimen from Soğanlı.

Figure 4. IRM component analysis by Kruiver et al. (2001) method. Data are fitted in three different graphics: on the left, a linear acquisition plot, LAP, in the middle, a gradient acquisition plot, GAP; on the right, a standardized acquisition plot, SAP. In (a) one magnetic component (Tilköy); in (b) two magnetic components (Yeşilöz); in (c) three magnetic components (Akköy). Symbols: dot = IRM data; thick solid line = sum of the individual components; long dash line: component 1; short dash line: component 2; thin short dash line: component 3.

Figure 5. B_{cr} and $S_{-0.3T}$ variation as a function of stratigraphic height. Grey area indicate the variability range for occurrence of low-coercivity ferrimagnetic component.

Figure 6. Plot of magnetic susceptibility versus density for each specimen.

Figure 7. Demagnetization results. Left: normalized intensity decay; middle: Zijderveld (1967) diagrams. Symbols: full/open dot = declination/apparent inclination; right: equal-area projection of demagnetization directions. Symbols: open dot = negative inclination.

Figure 8. Equal-area projection of the site mean paleomagnetic direction. Symbols: open dot = negative inclination; star = mean value and 95% confidence limit. In a) and b) the mean direction is computed by Fisher's (1953) statistics; in c) and d) by McFadden and McElhinny (1988) method; k = precision parameter; α_{95} = semi-angle of confidence.

Figure 9. Equal-areal projection of ChRM directions of representative sites (symbols as in figure 5) and the best-fit great circle and pole of the plane with confidence limit (McFadden and McElhinny, 1988). For each site the value of the pole direction and statistics parameters are indicated; ε = eccentricity (Engebretson and Beck, 1978).

Figure 10. Kizilkaya mean paleomagnetic direction (star and associated confidence limit) computed from site stable directions and site best-fitting circles (upper hemisphere projection). The direction of the GAD (grey square) and the directional value reported by Piper et al. (2002) (grey diamond), are drawn for comparison.

Figure 11. Magnetic declination and inclination variation as a function of sites' stratigraphic position at each locality. Vertical axes: GAD values at the sampling region (D = 0°, I = 58°); grey areas: locality mean declination and inclination confidence limit; horizontal bar: ΔD and ΔI values for sampling sites.

Table caption

Table 1. Paleomagnetic direction of the Kizilkaya ignimbrite. Symbols: n/N = number of specimens used for calculation/number of measured specimens; J_r = remanent magnetization intensity; D, I = magnetic declination and inclination; k = precision parameter; α_{95} = semi-angle of confidence; Statistics: M&M = McFadden and McElhinny (1988); F = Fisher (1953).

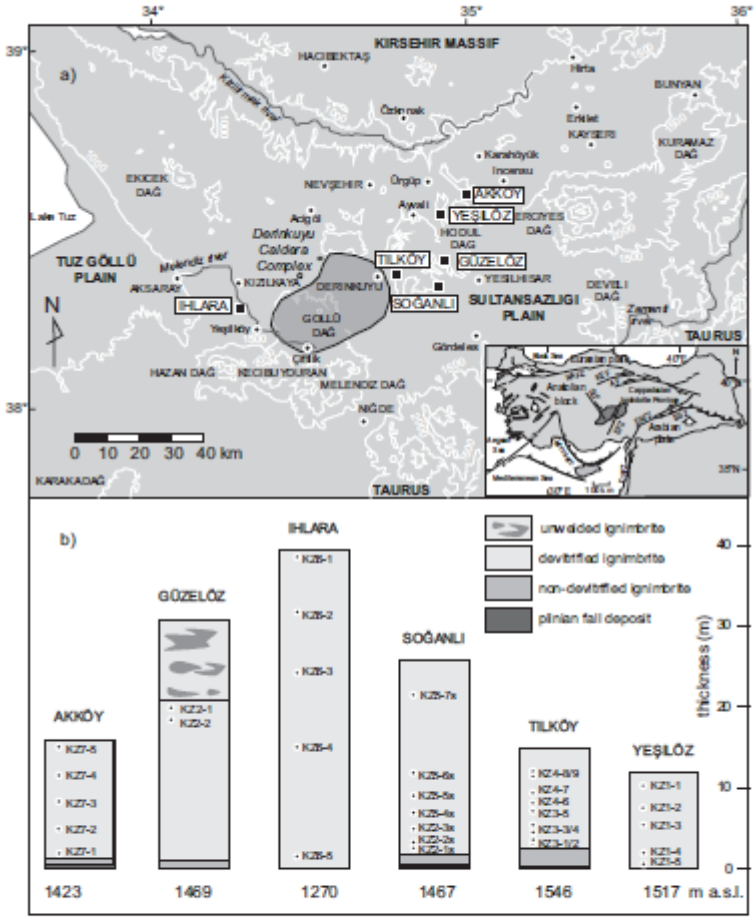

Figure 1

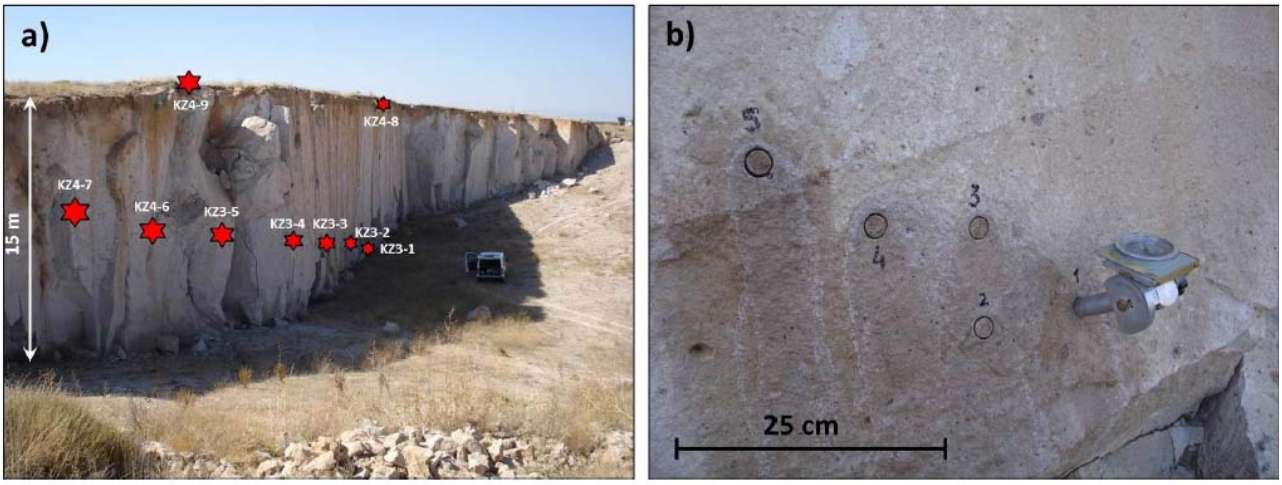

576
577 Figure 2

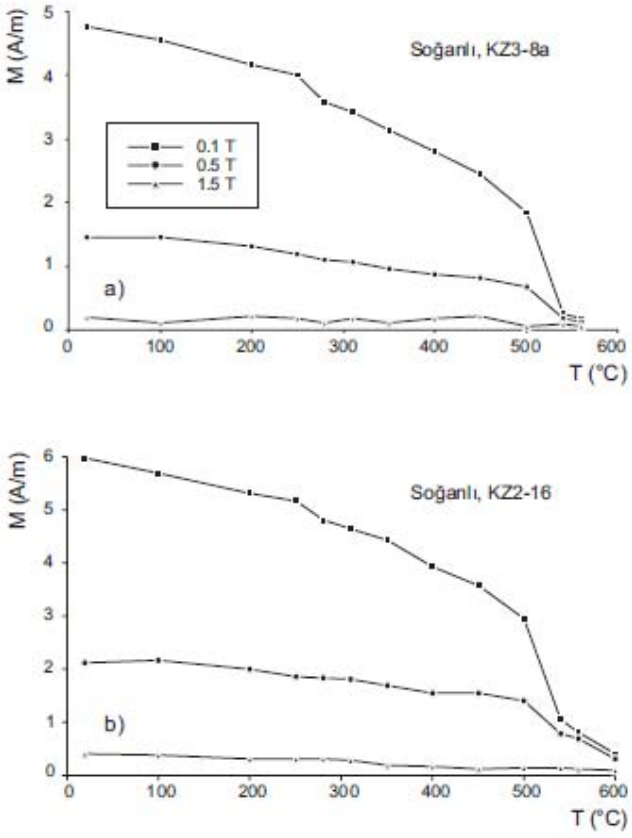

578
579 Figure 3

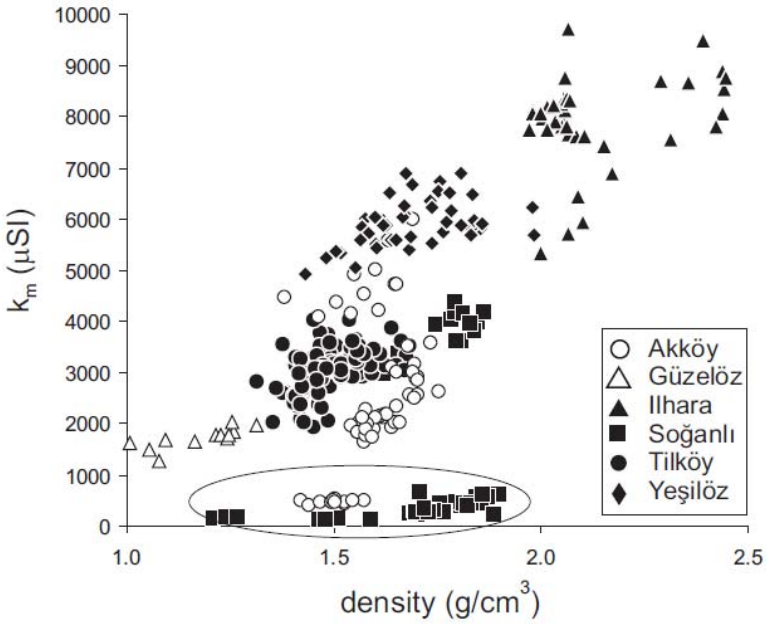

580

581 Figure 4

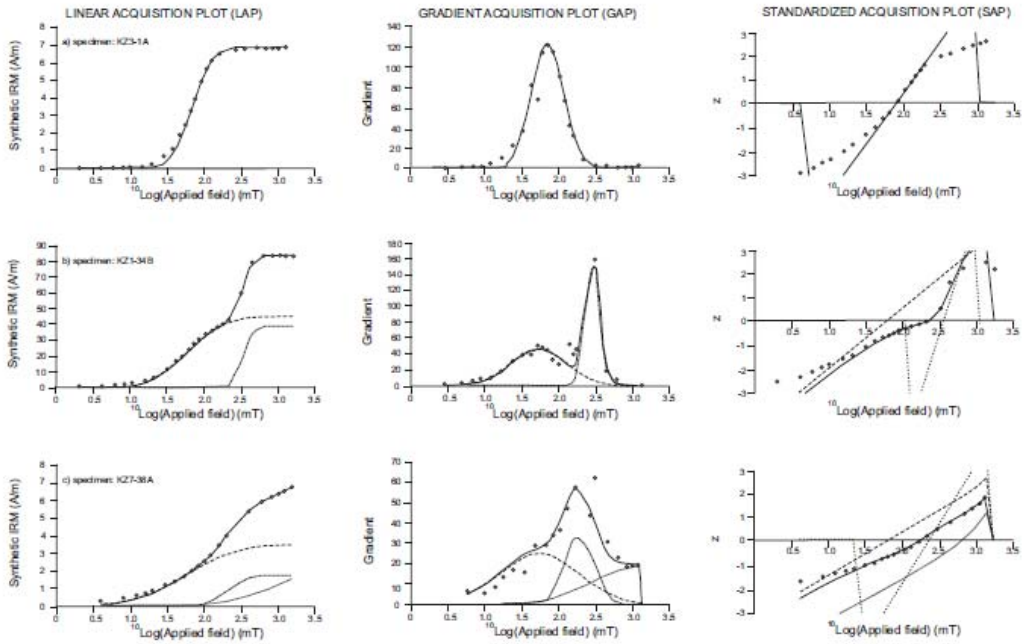

582
583 figure 5

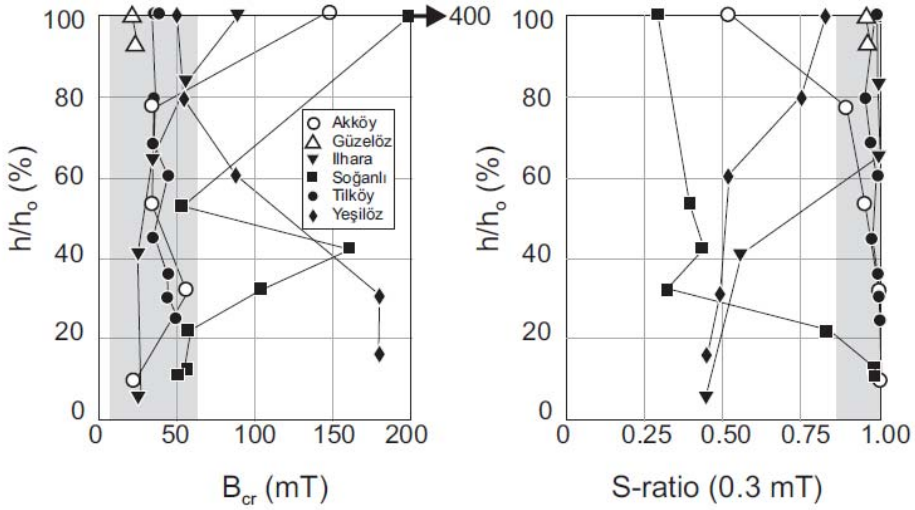

584
585 figure 6

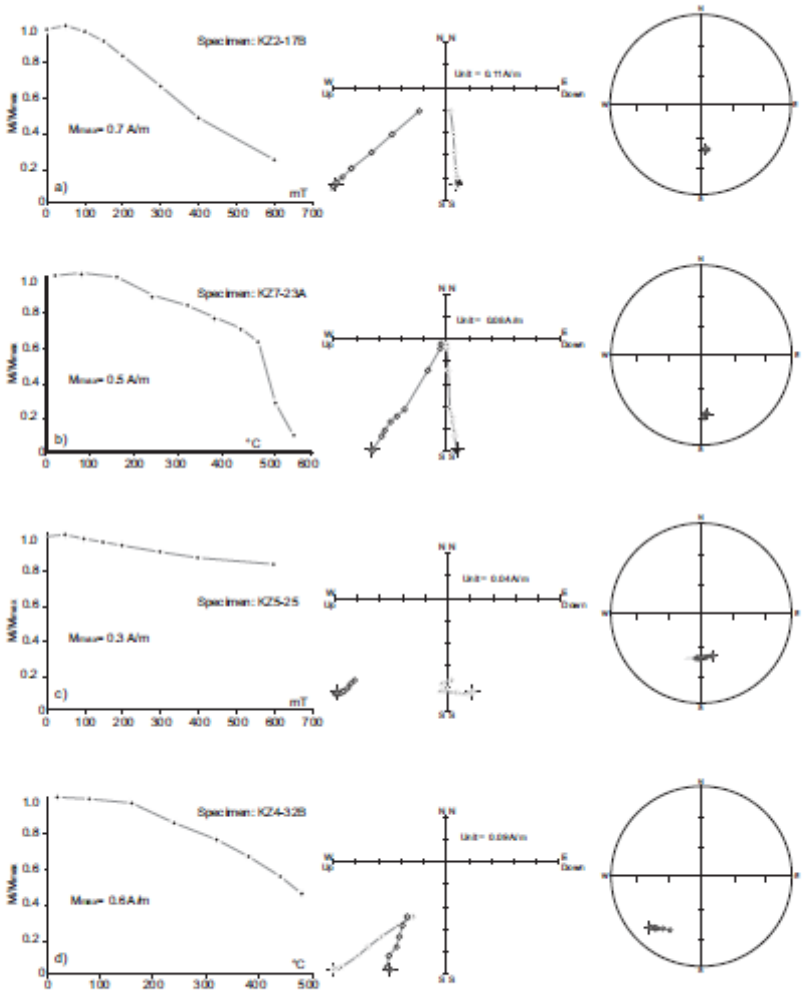

586

587 figure 7

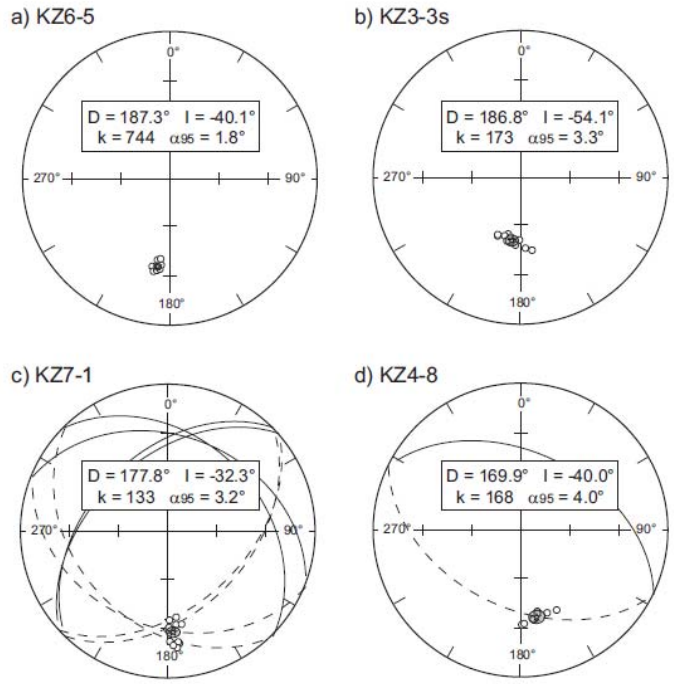

588

589 Figure 8

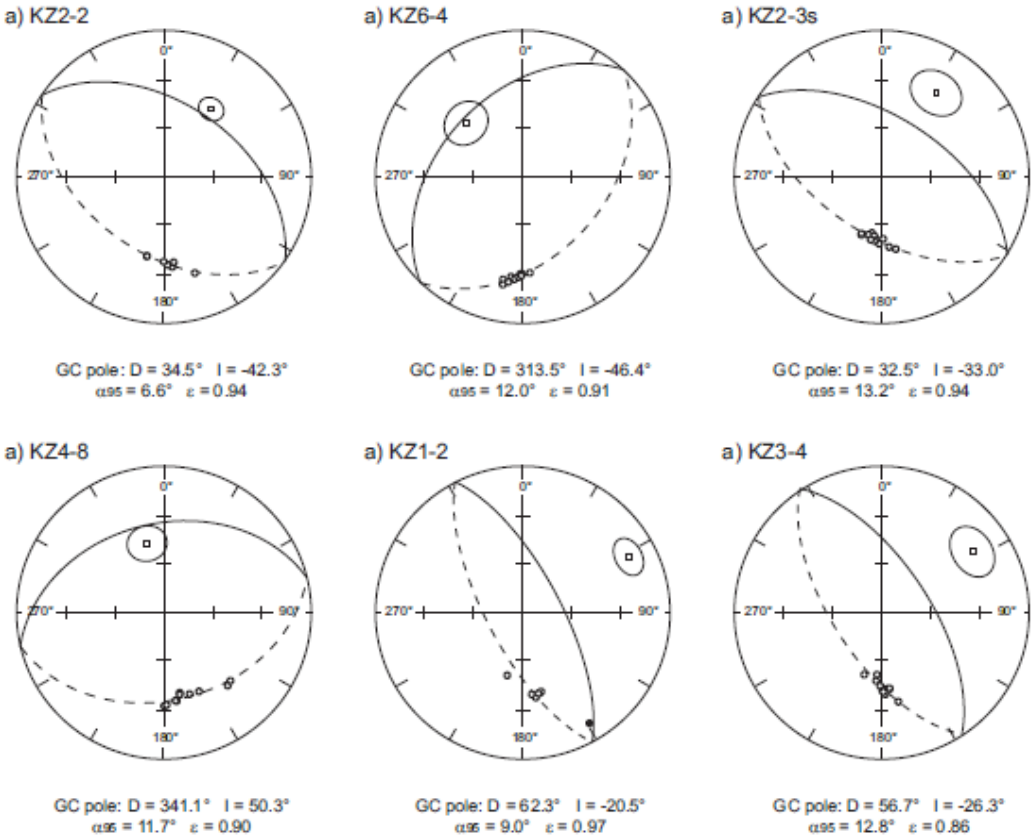

590

591 Figure 9

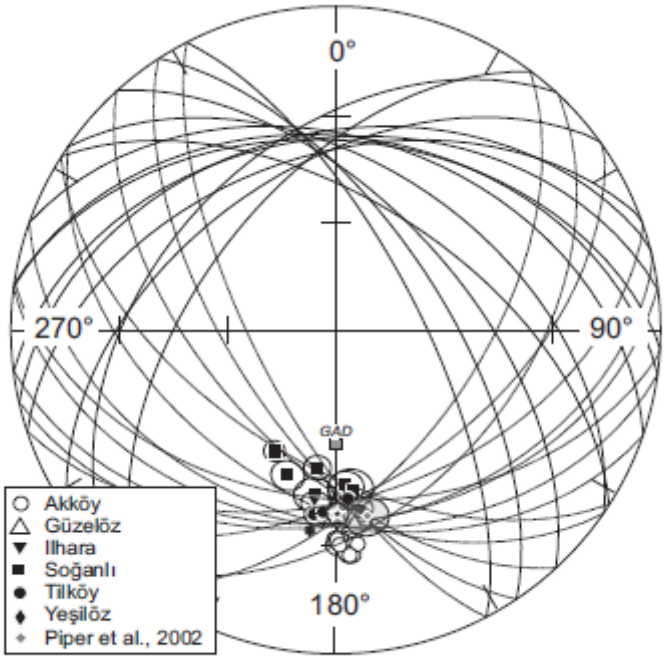

592

593 figure 10

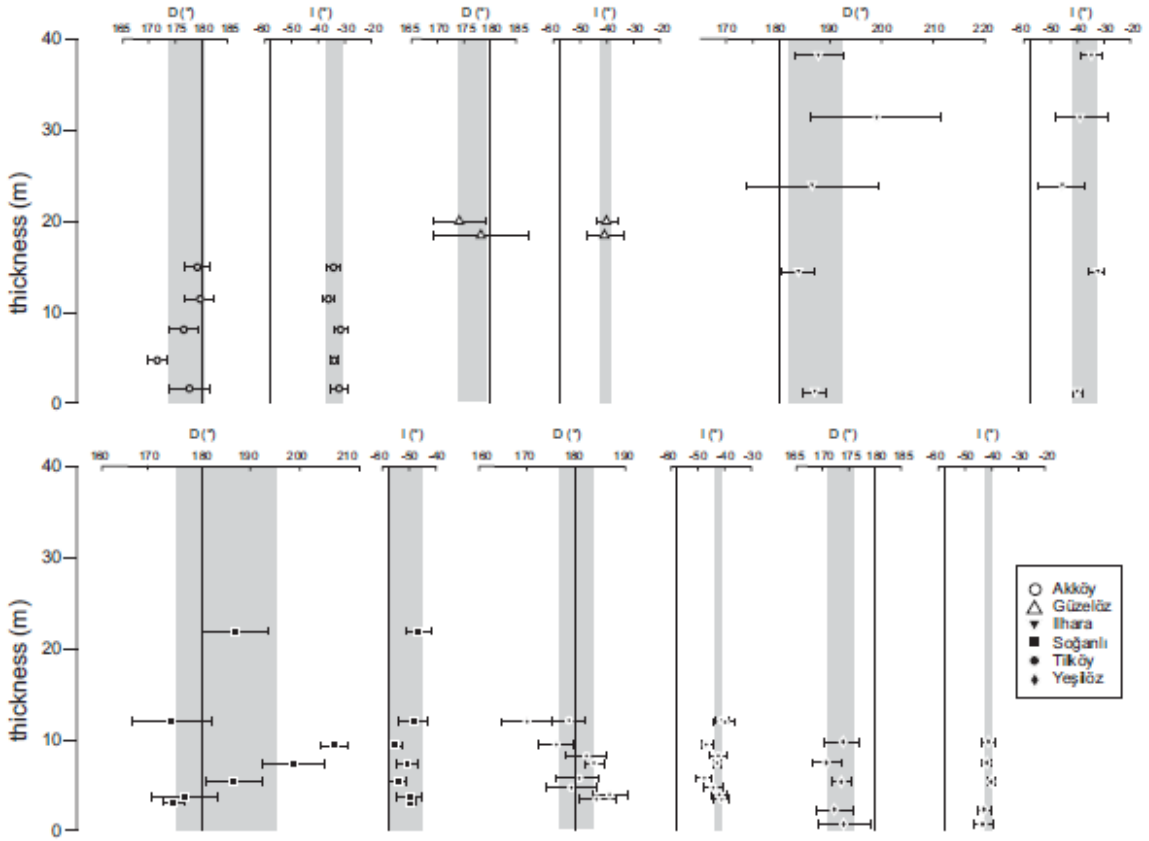

594

595 Figure 11

Locality	site	n/N	Jr	ChRM				Statistics
			A/m	D (°)	I (°)	k	α_{95}	
AKKÖY	KZ7-5	12/12	0.25	179.2	-34.5	438	2.1	M&M
	KZ7-4	12/12	0.40	179.8	-36.1	336	2.3	M&M
	KZ7-3	10/12	0.52	176.6	-31.5	377	2.3	M&M
	KZ7-2	12/12	0.47	171.6	-34.1	815	1.5	M&M
	KZ7-1	12/12	0.43	177.8	-32.3	133	3.2	M&M
GÜZELÖZ	KZ2-1	4/5	0.39	174.2	-40.7	558	3.9	F
	KZ2-2	7/7	0.43					
ILHARA	KZ6-1	6/6	0.88					
	KZ6-2	4/4	0.93					
	KZ6-3	4/5	2.43	186.7	-46.0	111	8.8	F
	KZ6-4	11/11	2.15					
	KZ6-5	10/12	2.10					
SOĞANLI	KZ5-7s	12/12	0.33	187.0	-46.6	148	4.7	M&M
	KZ5-6s	10/12	0.22	174.1	-48.4	292	5.4	F
	KZ5-5s	10/10	0.47	207.1	-55.4	337	2.6	F
	KZ5-4s	6/6	0.37	198.9	-50.7	280	4.0	F
	KZ2-3s	12/12	0.35					
	KZ2-2s	5/5	0.91	176.8	-50.1	458	4.3	F
	KZ2-1s	14/14	0.74	174.6	-49.4	789	1.4	F
TILKÖY	KZ4-9	11/11	0.64	178.5	-41.4	301	2.6	M&M
	KZ4-8	9/10	0.34					
	KZ4-7	13/13	0.50	175.8	-46.7	309	2.4	M&M
	KZ4-6	10/12	0.49	182.0	-42.6	283	3.2	F
	KZ3-5	9/13	0.47					
	KZ3-4	11/13	0.50					
	KZ3-3	12/12	0.41					
	KZ3-2	10/12	0.33	186.7	-42.2	243	2.7	F
	KZ3-1	10/12	0.34					
YEŞILÖZ	KZ1-1	5/6	1.71	173.7	-42.1	979	2.5	M&M
	KZ1-2	6/8	1.18					
	KZ1-3	11/15	1.61					
	KZ1-4	14/16	0.93	172.2	-43.3	266	2.6	M&M
	KZ1-5	7/11	0.89					

596

597 Table 1